High Resolution Magnetic Resonance Elastography of Glioblastoma Multiforme

Kaspar Josche Streitberger[1,2], Martin Reiß-Zimmermann[3], Karl-Titus Hoffmann[3], Florian Baptist Freimann[4], Felix Arlt[5], Jing Guo[1], Sebastian Hirsch[1], Jürgen Braun[6], and Ingolf Sack[1]

[1]Department of Radiology, Charité - Universitätsmedizin Berlin, Berlin, Berlin, Germany, [2]Department of Neurology, Charité - Universitätsmedizin Berlin, Berlin, Berlin, Germany, [3]Department of Neuroradiology, Universitätsklinikum Leipzig, Leipzig, Germany, [4]Department of Neurosurgery, Charité - Universitätsmedizin Berlin, Berlin, Berlin, Germany, [5]Department of Neurosurgery, Universitätsklinikum Leipzig, Leipzig, Germany, [6]Medical Informatics, Charité - Universitätsmedizin Berlin, Berlin, Berlin, Germany

Target audience: Physicians and basic scientists interested in the mechanical properties of soft tissues and tumors.

Background: Despite recent advances in operative and postoperative treatment, glioblastoma multiforme (GBM) still remains one of the most aggressive and malignant forms of cancer (1). Neuroradiological assessment of GBM and differentiation from solitary intracranial metastases or lymphomas is challenging due to the tumor's heterogeneous composition resulting from the presence of cysts, necrosis, and hemorrhage (2). Advanced MRI methods such as DTI provide structural information related to water mobility in white matter tracts but cannot reveal the consistency and mechanical constitution of biological tissue (3). Targeting the mechanical properties of intracranial tumors by MR elastography (MRE) (4) could provide new information for an improved treatment planning, and therapy monitoring.

Purpose: To generate high resolution maps of the mechanical consistency of the human brain for the presurgical quantification of viscoelastic properties of GBM.

Methods: 17 patients with GBM were included in this study. 9 patients were investigated in a 3T and 8 patients in a 1.5-T system. A spin echo EPI sequence with flow compensated motion encoding gradient was used. 7 vibration frequencies (30 to 60 Hz with 5 Hz increment) were induced by a nonmagnetic driver mounted to a head cradle. For 10 (1.5T) and 15 (3T) adjacent slices of 2x2x2 mm3 resolution, 7 frequencies, 8 wave dynamics, and 3 encoding directions were applied. Total acquisition time was ca. 9 min. For data processing, gradient-based unwrapping was performed followed by multifrequency inversion of all first order in-plane derivatives of the wave field (5) resulting in two independent constants, |G*| and φ, corresponding to the magnitude and phase of the complex shear modulus G*.

Pat.	Morphology	Localization
1	mostly solid tumor	parietal (l)
2	mostly solid tumor, few cysts	temporal (l)
3	solid tumor with central necrosis	parietal (l)
4	large central necrosis with hemorrhages	parietooccipital (l)
5	mostly solid tumor with cysts	temporooccipital (r)
6	mostly solid tumor	CC (b)
7	many small cysts, no hemorrhage	frontal (r)
8	large central hemorrhage	frontal (r)
9	solid tumor with small cystic fraction	parietal+ventricle (r)
10	indistinct tumor edge with necrotic fraction, only few cysts and solid parts	frontotemporal (l)
11	mostly solid tumor with central necrosis, no cysts, no hemorrhage	parietooccipital (l)
12	diffuse tumor with few solid fractions	parietal (l)
13	mostly solid tumor with descrete zentral necrosis, no cysts	occipital, CC (r)
14	cystic tumor, no hemorrhage	frontal (b)
15	tumor with central necrosis and hemorrhages, only little solid appearing mass	temporal (r)
16	mostly solid tumor, few cysts, discrete hemorrhage	occipital (r)
17	mostly cystic, solid tumor rostral, discrete hemorrhage	frontal (r)

Tab.1: Morphological classification and localization of all GBM included in this study

Results: Morphological tumor assessment and tumor locations are stated in Tab.1. MRE parameter maps of |G*| and φ are shown in Fig.2 for two cases with stiff and soft GBM. On average, a mean |G*| value of 1.30 ± 0.26 kPa was measured in GBM, while healthy tissue was significantly stiffer than GBM with a mean value of 1.50 ± 0.25 kPa (P = 0.008). In 4 tumors |G*| was higher than healthy reference tissue (P = 0.03). Mean φ was 0.38 ± 0.09 for GBM and 0.58 ± 0.08 for the corresponding healthy tissue. Ratios GBM/reference tissue of |G*| and φ are shown in Fig.3. 13 GBM in our study presented with extended perifocal edema. Edematous tissue had higher |G*| values than GBM (P = 0.014) while φ was not altered.

Discussion: This study presents high resolution MRE of intracranial tumors. The reconstructed MRE parameters |G*| and φ are similar to parameters given in (6), however, by a much better spatial resolution due to the inclusion of multiple drive frequencies, enabling us for the first time to analyze the intrinsic heterogeneities of tumors. Interestingly, in 4 out of 17 cases GBM was stiffer than healthy tissue while reduction in φ was seen in all tumors (P = 1.3 x 10-7) suggesting less dissipative GBM properties consistent with previous findings in different tumor entities (6).

Conclusion: In average GBM are softer and less dissipative than healthy brain tissue. Unrelated to morphological markers, MRE provides an entirely new neuroradiological contrast related to the biomechanical properties of tumors as encountered by surgeons during interventions.

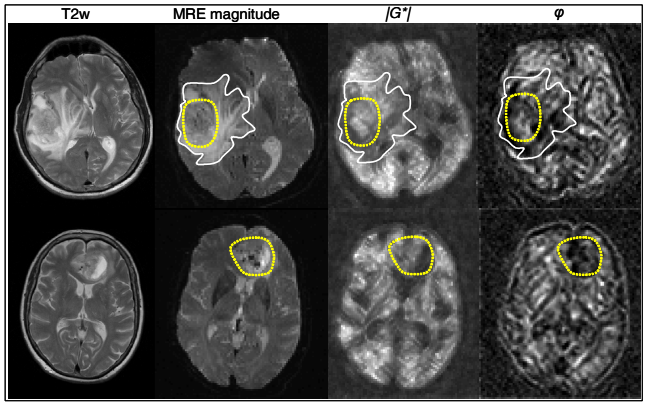

Fig.2: Anatomical images, and MRE parameter maps of 2 GBM patients (upper row: patient #15, bottom row: patient #14, corresponding to the table).

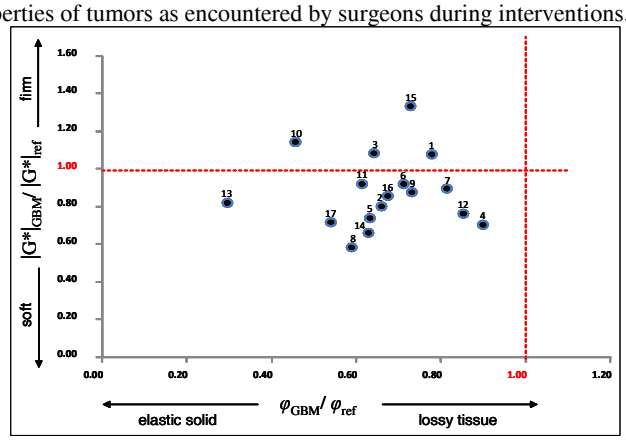

Fig.3: Viscoelastic properties of GBM based on the parameter ratios of |G*| and φ between tumor and healthy reference tissue (ref).

References: 1. Furnari et al. *Genes & Development* 2007;21:2683-2710. 2. Toh et al. *AJNR* 2011;32:1646-1651. 3. Johnson et al. *Neuroimage* 2013; 79:145-152. 4. Murphy et al. *Journal of neurosurgery* 2013;118:643-648. 5. Guo et al. *PLOSONE* 2013;8:e71807. 6. Simon et al. *The New Journal of Physics* 2013;15:085024